Cancer Research

A Three-Dimensional Organoid Culture System Derived from Human Glioblastomas Recapitulates the Hypoxic Gradients and Cancer Stem Cell Heterogeneity of Tumors Found *In Vivo*

Christopher G. Hubert[1], Maricruz Rivera[1], Lisa C. Spangler[1], Qiulian Wu[1], Stephen C. Mack[1], Briana C. Prager[1], Marta Couce[2], Roger E. McLendon[3], Andrew E. Sloan[4], and Jeremy N. Rich[1]

Abstract

Many cancers feature cellular hierarchies that are driven by tumor-initiating cancer stem cells (CSC) and rely on complex interactions with the tumor microenvironment. Standard cell culture conditions fail to recapitulate the original tumor architecture or microenvironmental gradients and are not designed to retain the cellular heterogeneity of parental tumors. Here, we describe a three-dimensional culture system that supports the long-term growth and expansion of tumor organoids derived directly from glioblastoma specimens, including patient-derived primary cultures, xenografts, genetically engineered glioma models, or patient samples. Organoids derived from multiple regions of patient tumors retain selective tumorigenic potential. Furthermore, organoids could be established directly from brain metastases not typically amenable to *in vitro* culture. Once formed, tumor organoids grew for months and displayed regional heterogeneity with a rapidly dividing outer region of $SOX2^+$, $OLIG2^+$, and TLX^+ cells surrounding a hypoxic core of primarily non-stem senescent cells and diffuse, quiescent CSCs. Notably, non-stem cells within organoids were sensitive to radiotherapy, whereas adjacent CSCs were radioresistant. Orthotopic transplantation of patient-derived organoids resulted in tumors displaying histologic features, including single-cell invasiveness, that were more representative of the parental tumor compared with those formed from patient-derived sphere cultures. In conclusion, we present a new *ex vivo* model in which phenotypically diverse stem and non-stem glioblastoma cell populations can be simultaneously cultured to explore new facets of microenvironmental influences and CSC biology. *Cancer Res; 76(8); 2465–77. ©2016 AACR.*

Introduction

Glioblastoma patient prognosis is dismal with a median patient survival of 14 to 16 months (1). Our inability to effectively treat glioblastomas is due, in part, to their great heterogeneity on both the cellular and microenvironmental levels (2–4). Glioblastoma growth may be governed by stochastic or hierarchical models (5), and although these models are not mutually exclusive, recent studies suggest the presence of self-renewing, tumor-propagating cancer stem cells (CSC; refs. 6–8). While CSCs remain controversial due to unresolved issues of enrichment markers, functional assays, and cellular origin, the importance of these cells has been supported by findings that CSCs are resistant to conventional therapies due to multiple mechanisms, including increased DNA repair (9).

Glioblastoma is a hierarchically organized cancer where stem-like tumor cells receive critical maintenance cues from their microenvironment. CSCs reside in perivascular niches where close proximity to the vasculature provides nutrients and oxygen (10). A second stem-like tumor cell population resides in hypoxic regions distal to the vasculature (11–13). Tumor stem, non-stem, and normal cells engage in bidirectional communication to provide instructional cues for the maintenance of cell state (14–16). Differentiated progeny and blood vessels stimulate CSC maintenance through production of cytokines (17), nitric oxide (15), Notch ligands (16), and extracellular matrix (2). CSCs are not passive recipients of microenvironmental cues, as CSCs stimulate angiogenesis through proangiogenic growth factor signaling (18), direct the differentiation of progeny (14), and possess lineage plasticity toward vascular pericytes (19). The CSC state is, therefore, plastic and can be influenced by the cellular microenvironment, contributing to the concept of both cell autonomous and extrinsically instructed CSCs.

Interrogating tumor cell–microenvironmental interactions is challenging. Genetically engineered mouse models are highly valuable resources but can also differ from human tumors due to species-specific distinctions and comparatively rapid evolution

[1]Department of Stem Cell Biology and Regenerative Medicine, Lerner Research Institute, Cleveland Clinic, Cleveland, Ohio. [2]Department of Pathology, University Hospitals Case Medical Center, Cleveland, Ohio. [3]Department of Pathology, Duke University Medical Center, Durham, North Carolina. [4]Center for Brain Tumor and Neuro-Oncology, Department of Neurological Surgery, Neurological Institute and Seidman Cancer Center, Case School of Medicine, University Hospitals Case Medical Center, Cleveland, Ohio.

Note: Supplementary data for this article are available at Cancer Research Online (http://cancerres.aacrjournals.org/).

M. Rivera and L.C. Spangler contributed equally to this article.

Corresponding Author: Jeremy N. Rich, The Cleveland Clinic, 9500 Euclid Avenue, Cleveland, OH 44195. Phone: 216-636-0790; Fax: 216-636-5454; E-mail: drjeremyrich@gmail.com

doi: 10.1158/0008-5472.CAN-15-2402

of the mouse tumors. For human models, the most accurate way to study tumor cell and environmental interactions is orthotopically *in vivo*, but this preservation of complexity also dramatically limits experimental control (20). To ask questions *in vitro*, researchers must select the desired culture conditions. Due to precedence and convenience, these conditions are generally not representative of tumor conditions in patients (i.e., atmospheric oxygen, neutral pH, superphysiologic glucose concentration, etc.). This choice influences and standardizes cellular responses, complicating experimental separation of instructive cues by intrinsic networks versus those generated by the culture environment. As culture selects cells to a relatively uniform state, it has been impossible to study long-term relationships of different cell populations growing together as they occur in a tumor. CSCs and non-stem tumor cells are generally maintained under incompatible conditions, complicating studies of crosstalk. Hypoxic cell culture using separate controlled incubators also precludes study of hypoxic–nonhypoxic cell interactions.

Recently described three-dimensional culture methods recapitulate features of *in vivo* cell growth, allowing self-organization, differentiation, and mixed heterogeneity to exist within the culture environment (21–29). Here, we describe a novel organoid culture system using patient-derived glioblastoma CSCs that recapitulates hypoxic gradients and stem cell heterogeneity found in tumors *in vivo*. Such gradients are not possible using current culture methods. This system will allow the study of heterogeneous cell–cell relationships, including the coculture of hypoxic and nonhypoxic CSCs.

Materials and Methods

Human cell and organoid culture

Glioblastoma samples were obtained directly from patients undergoing resection in accordance with protocol #2559 approved by the Cleveland Clinic Institutional Review Board. Patient tissue samples were either finely minced prior to organoid formation or were dissociated into single-cell suspensions, red blood cells removed by brief hypotonic lysis, and counted for cell number and viability using trypan blue. All cells used in this work, with the exception of the mouse-derived RCAS-GFAP-tva/PDGFB cell culture, were patient-derived primary cultures, and all specimens were verified by comparison of short tandem repeat analysis performed both immediately after isolation and periodically during the course of experimentation. Tumorspheres were maintained as xenografts and harvested for culture as previously described (9). Xenografts were dissociated (Tumor dissociation kit #130-095-929; Miltenyi), magnetically sorted for CD133 (CD133 beads; Myltenyi; IN528 and 387 cells only), and were cultured as tumorspheres in Neurobasal medium supplemented with EGF (R&D Systems), bFGF (R&D Systems), B27 (Invitrogen), glutamine (CCF media core), sodium pyruvate (Invitrogen), and antibiotics (Anti-anti; Invitrogen), termed "NBM complete." No cells were propagated more than 5 passages in culture after isolation.

Briefly, organoids were formed by suspending tumor cells in Matrigel and forming 20 μL pearls on parafilm molds prior to culture. Organoids were cultured in 6-well or 10-cm plates, shaking in NBM complete media. Images of growing organoids were acquired using an EVOS FL Cell Imaging System (Invitrogen) for microscopic imaging, or a handheld Samsung Galaxy S4 for macroscopic imaging (please see Supplementary Methods S1 for detailed organoid procedures).

Mice

All experiments involving mice were approved by the Cleveland Clinic Institutional Animal Care and Use Committee (IACUC). All methods and experiments were carried out in accordance with the approved relevant guidelines and regulations under IACUC protocol #2013-0935. For *in vivo* tumor formation studies, whole organoids were minced, dissociated (tumor dissociation kit; #130-095-929; Miltenyi), counted, and 50,000 cells were orthotopically xenografted into the right cortex of immunodeficient NOD.Cg-Prkdc^{scid} Il2rg^{tm1Wjl}/SzJ (NSG) mice. Mice were sacrificed upon display of overt phenotypic or neurological signs.

Immunofluorescence and imaging

Briefly, whole organoids were fixed, snap-frozen in Tissue-Tek O.C.T. optimal cutting temperature compound (VWR), and sectioned at 10 μm before being probed with antibodies for immunofluorescence. DNA was detected using DAPI (1:10,000) or DRAQ5 (Invitrogen; 1:1,000). Images were acquired using a Leica DM4000 B upright fluorescent microscope, and mosaic images were assembled by hand using Adobe Photoshop (please see Supplementary Methods S1 for antibody lists and additional details).

Results

Establishment of glioblastoma organoids

Glioblastoma tumors contain variable regions of comparatively high oxygenation and nutrient levels in the perivascular space, changing to nutrient-poor, hypoxic, and necrotic regions distal to the vasculature (10, 30). Organoids can grow beyond this size and are viable well in excess of observed diffusion limits. We reasoned that by utilizing organoid culture methods, we could establish CSC cultures with mixed regions of oxygen-high, nutrient-high regions as well as chronic hypoxic and necrotic areas.

To initiate glioblastoma organoids, we modified an original procedure developed for cerebral organoids (Supplementary Methods S1; refs. 25, 26). For comparison, we grew parallel CSCs with identical media (NBM complete) and media replacement schedules either (i) in traditional serum-free sphere culture (Fig. 1A–C, H), or (ii) as three-dimensional organoids (Fig. 1D–F). Whereas standard tumorspheres reached a maximum size of approximately 300 μm within 2 weeks, organoids expanded prolifically to a size of approximately 3 to 4 mm after 2 months (Fig. 1G). Establishment of viable organoids was effective from primary cultures using either whole tumorspheres or dissociated CSCs embedded in Matrigel (data not shown). After several months, isolated single organoids generated smaller, daughter spheres in culture, which could subsequently fuse to the main organoid. Although growth rates notably slowed over several months of culture, glioblastoma organoids can be stable and viable after more than a year of continuous culture without passaging (Figs. 1I, J and 2A). Organoids can further be established from specimens of human origin and from genetically engineered glioma mouse models (Supplementary Fig. S1A–S1D), allowing potential transgenic studies in organoids.

Growth of tumorigenic organoids directly from primary patient samples

Avatars created from patient tumors may predict response to therapy (31). The ability to establish primary patient-derived xenografts and primary cultures from surgical specimens remains

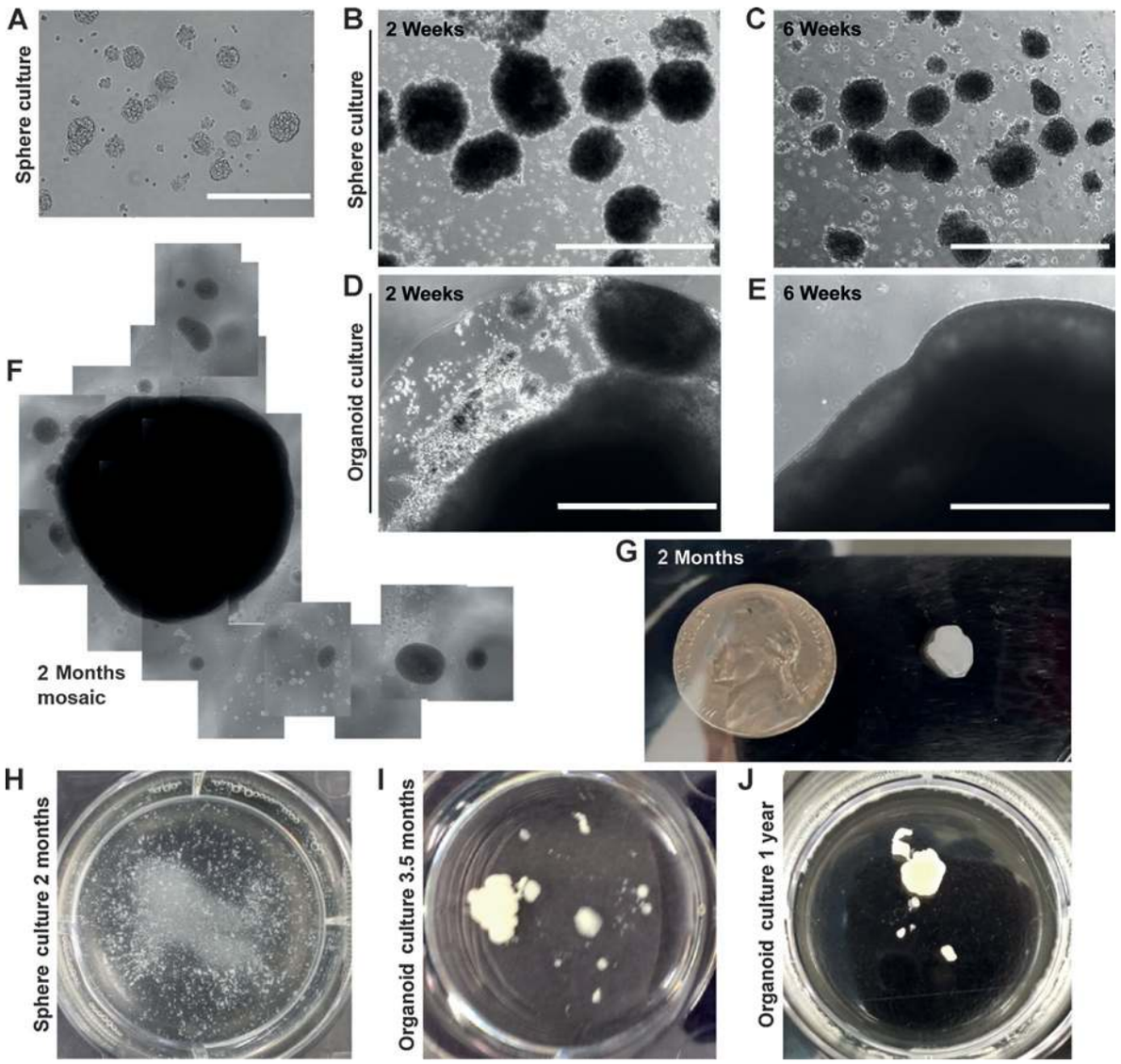

Figure 1.
Establishment of glioblastoma CSC organoids. A, micrograph of IN528 tumorspheres; scale bar, 400 μm. B–E, parallel IN528 tumorsphere (B, C) or organoid cultures (D, E) for 2 and 6 weeks; scale bar, 1000 μm. F, mosaic image of multiple low-power (4×) microscope fields showing organoid growth and smaller satellite spheres. G, IN528 organoid prior to embedding and sectioning. US nickel for scale. H–J, images of 6-well plate wells containing IN528 tumorspheres (H) or organoids (I, J) at indicated time points.

a biologic, technical, and logistical barrier in tumor research. We therefore investigated whether glioblastoma organoids could be grown directly from patient tumor tissues. Fresh surgical specimens were finely minced, diluted with culture media, and mixed with Matrigel to form organoids as described above (Fig. 2A). After several months of culture, we functionally quantified the stem cell population and putative tumor-initiating capabilities of these organoids using limiting dilution assays. The organoids contain sphere-forming CSCs at rates similar to, though slightly lower than, tumorspheres (Fig. 2B). After 5 to 6 months of growth, single organoids were dissociated and orthotopically implanted into the frontal lobes of mice, which were then monitored. All recipient mice succumbed to brain tumors, with an average latency of approximately 2 months (Fig. 2C), demonstrating that primary patient cells can proliferate and retain their tumorigenic potential after months of organoid culture. In comparison, the same number of tumorsphere cells established intracranial xenografts much more rapidly, with a latency of 2 weeks (Fig. 2C). The conditions of tumor cell propagation prior to xenograft therefore greatly alter the growth phenotype of the subsequent xenograft tumors.

Organoids recapitulate single-cell tumor invasion *in vivo*

Although the CCF3128 tumorspheres and organoids have similar proportions of functional sphere-forming cells, xenografts derived from these sources had very different latencies. Compared with tumorspheres, organoid cultures contained marked

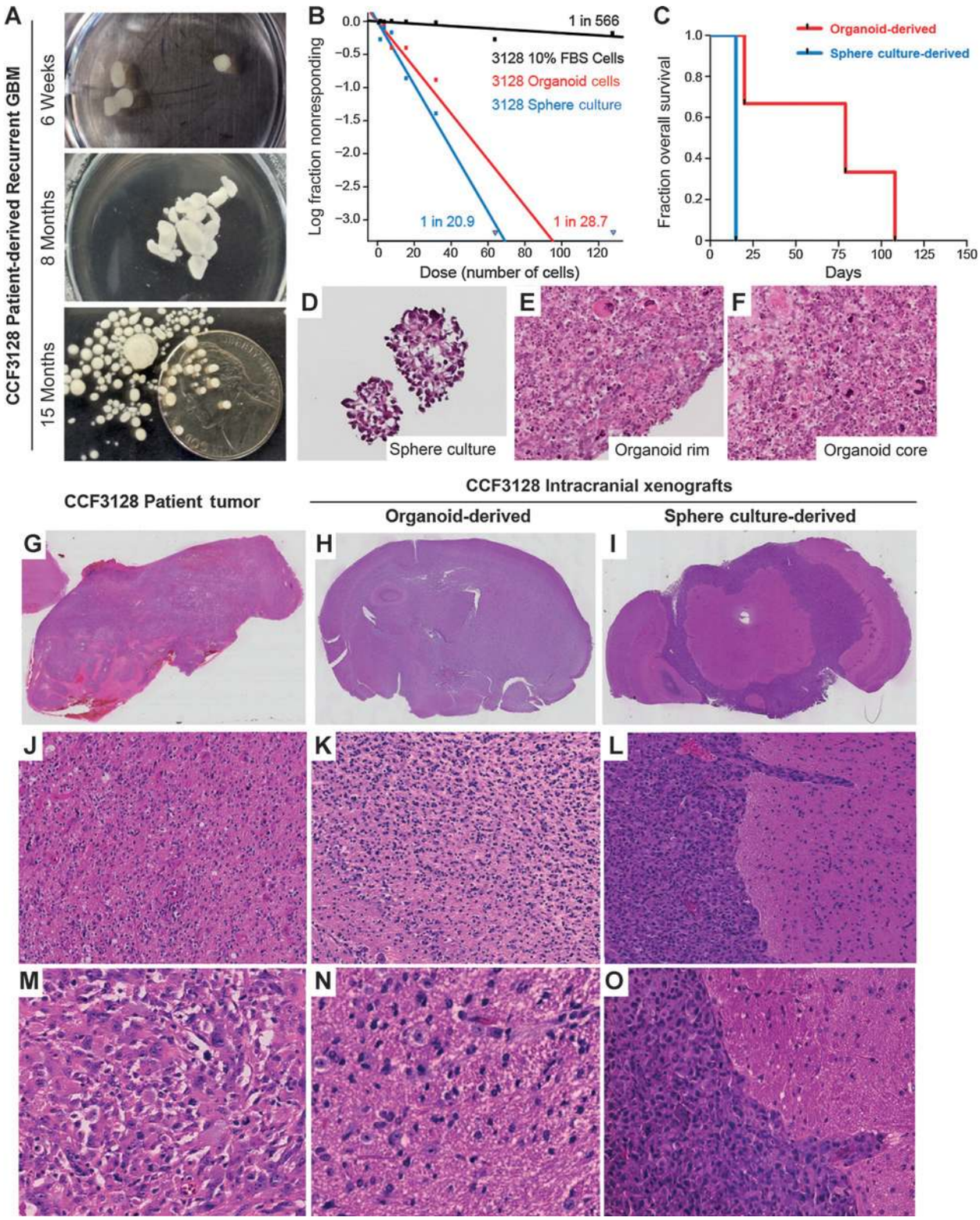

Figure 2.
Organoid-derived glioblastoma xenografts recapitulate the diffusive phenotype of the original patient tumor. A, longitudinal growth of CCF3128 patient-derived recurrent glioblastoma in organoid culture. B, limiting dilution assays of organoid, tumorsphere, or FBS-differentiated CCF3128 cells. Sphere-forming cell frequencies are indicated next to each line. C, survival plot of mice following orthotopic injection of 50,000 dissociated CCF3128 organoid or tumorsphere cells. D–F, high-power micrographs of tumorsphere or organoid-frozen sections (hematoxylin and eosin, H&E; 40×). (*Continued on the following page.*)

pleomorphism in both the core and rim regions with significant variability in size, nuclear morphology, and cytologic features (Fig. 2D–F). This led us to investigate the histologic variation of the resulting xenografts (Fig. 2G–O). Xenografted CCF3128 tumorsphere cells exhibited a solid growth pattern (Fig. 2I, L, O) as is common for glioblastoma xenografts. In contrast, glioblastoma patient tumors are often highly diffuse and infiltrative. The original CCF3128 patient specimen displayed a clear single-cell infiltrative phenotype, a diffuse tumor cell growth pattern, and tumor cells with eosinophilic cytoplasm (Fig. 2G, J, M). This pattern was maintained in mouse orthotopic xenografts derived from CCF3128 organoid cultures (Fig. 2H, K, N). Our results demonstrate that the frequent loss of a specimen's diffuse invasive phenotype upon culture and subsequent xenograft may not be simply due to a predisposition of the patient sample or to the xenograft format *per se*, but can be a result of the cell expansion conditions prior to xenograft. Expansion of samples as organoids can preserve this phenotype.

Organoid creation from brain metastases

Brain metastases can be a devastating consequence of numerous cancer types; however, patient-derived brain metastases are notoriously difficult to culture *in vitro*. We tested in parallel whether tumorsphere or organoid culture could support the growth of a patient brain metastasis sample from esophageal adenocarcinoma. As observed historically, the brain metastasis failed to grow as spheres (Supplementary Fig. S2A). In contrast, niduses of cell growth became apparent in multiple organoids and expanded to comprise the complete organoid matrix within 5 weeks (Supplementary Fig. S2B). Thus, organoid culture enables the growth and study of tumor specimens that would otherwise be lost.

Derivation of organoids from multiple tumor regions

In addition to cell-type heterogeneity, glioblastomas demonstrate remarkable regional heterogeneity in radiographic imaging and histology (32). Selection bias in the establishment of *in vitro* cultures from clinical samples can therefore be a product of the sample site of the original tumor combined with how the sampled cells will propagate under given culture conditions. Organoid culture, however, may intrinsically contain microenvironmental gradients permissive for the settling and outgrowth of tumor cell populations from diverse tumor environments.

To determine whether organoid culture allows the growth of samples from varying tumor regions, we isolated samples from three spatially distinct patient tumor regions based on MRI imaging: the potentially invasive FLAIR region, the contrast-enhanced tumor zone, and the inner necrotic/hypoxic core (Fig. 3A). Samples from each respective region were pathologically diagnosed as infiltrating high-grade astrocytoma (CW1757.1; Fig. 3B), high-grade astrocytoma with scant necrosis (CW1757.2; Fig. 3C), and high-grade astrocytoma with necrosis, gliosis, and possible treatment effect (CW1757.3; Fig. 3D).

Samples from each region were macrodissected, finely minced, and cultured as organoids. Within 2 weeks, cells from all three regions visibly invaded the Matrigel, filling its boundaries by 7 weeks and growing stably for months (Fig. 3E). To evaluate tumor initiation capability after organoid culture, we dissociated and orthotopically xenografted organoids from each region. Although all three regions were cultured identically, cells derived from the necrotic tumor core reinitiated tumors dramatically faster than the other two regions (Fig. 3F). Cells with tumorigenic potential were maintained from all regions, but the stark contrast between region 3 and regions 1 and 2 demonstrates that organoids maintain functionally divergent tumor cell populations from distinct tumor regions. These organoid-derived xenografts also demonstrated marked heterogeneity and reproduced the indistinct margins and single-cell infiltration present in the original patient sample (Fig. 3G–I), reflecting the results from the organoid-derived CCF3128 xenografts above (Fig. 2H, K, N). Organoids therefore represent a new tool for the growth and maintenance of diverse tumor populations, including infiltrative cells, *in vitro*.

Tumor organoids generate gradients of stem cell density and hypoxia

Limitations in oxygen and nutrient availability stimulate glioblastoma self-renewal and promote maintenance of a stem-like cell state (11, 33). We therefore hypothesized that organoids would have spatial differences in the populations of stem-like and differentiated cell populations present. SOX2 is a transcription factor highly associated with pluripotency (34), a Yamanaka factor capable of iPS cell reprograming (35), and a well-described marker of glioma CSCs (36, 37). Glioma CSC tumorspheres almost universally express SOX2, limiting the ability to study heterogeneous populations simultaneously. We performed immunofluorescent analysis of SOX2 to visualize CSC localization in organoids from three independent patient tumor specimens. SOX2 expression was notably denser near the periphery of each organoid and transitioned to punctate staining deeper in the core (Fig. 4A–C). Organoid centers often contained a mix of noncellular areas filled with fluid or extracellular matrix, and cellular areas with a mix of both stem and non-stem cells spread throughout. Cells near the edges of the organoids were almost uniformly stem-marker positive, perhaps due to the proximity to stimulatory growth factors (EGF, bFGF). These patterns were stable at various time points (Supplementary Fig. S3A–S3C) including after many months (Fig. 4C).

(*Continued.*) G, low-power micrograph of biopsy sample (H&E; 1×). H, whole mount mouse brain bearing organoid-derived xenograft demonstrating effacement of ventricles and asymmetric expansion of cerebral hemispheres with no clear margins of tumor (H&E; 1×). I, whole mount mouse brain bearing tumorsphere-derived xenograft showing solid growth pattern in subarachnoid space and clear margins of tumor/brain interface. (H&E; 1×). J, intermediate power micrograph of patient biopsy specimen exhibiting a diffuse growth pattern of tumor cells with eosinophilic cytoplasm (H&E; 10×). K, intermediate power micrograph of organoid-derived xenografted tissue showing a diffuse growth pattern of tumor cells with eosinophilic cytoplasm and irregularly shaped nuclei (H&E; 10×). L, intermediate power micrograph of tumorsphere-derived xenograft showing solid growth pattern, sharp tumor–brain interface with tumor cells growing down a perivascular Virchow–Robin space (H&E; 10×). M, high-power micrograph of patient biopsy tissue exhibiting variable amounts of eosinophilic cytoplasm with hyperchromatic irregular nuclei and pleomorphic cytoplasmic outlines (H&E; 40×). N, high-power micrograph of organoid-derived xenografted tissue exhibiting individual fibrillar tumor cells infiltrating into the brain substance as single cells with variable amounts of intervening brain parenchyma between the pleomorphic tumor cells (H&E; 40×). O, high-power micrograph of tumorsphere-derived xenografted tissue showing solid growth pattern of basophilic tumor cells with high nuclear to cytoplasmic ratios that exhibit a sharp tumor–brain interface with infiltration along the perivascular Virchow–Robin space (H&E; 40×).

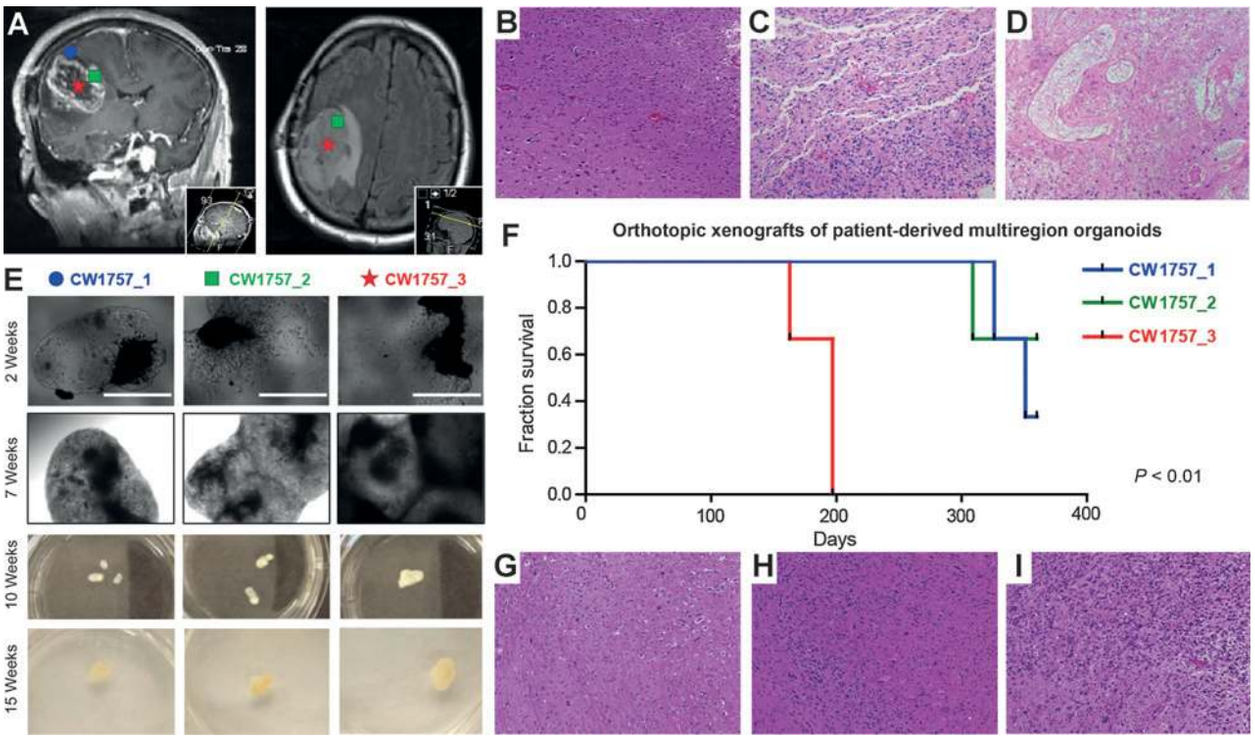

Figure 3.
Patient-derived multiregion tumor samples. A, based on preoperative MRI scans, surgical samples were selected from three distinct tumor regions for laboratory propagation. These regions were: CW1757_1 = superficial cortex ≥ 3 mm from enhancing margin and also within hyperintense FLAIR; CW1757_2 = enhancing margin of tumor; CW1757_3 = tumor center, hypointense on T1 and nonenhancing (typically associated with necrosis on IHC). B, high-power micrograph of CW1757_1 patient-derived biopsy tissue along the tumor–brain margin demonstrating mild increase in cellular density related to single-cell infiltration of tumor cells (hematoxylin and eosin, H&E; 40×). C, high-power micrograph of CW1757_2 biopsy demonstrating markedly increased fibrillar tumor cellular density with variable amounts of intercellular eosinophilic brain parenchyma and no geographic necrosis (H&E; 40×). D, high-power micrograph of CW1757_3 biopsy demonstrating regions of geographic necrosis (centrally), consistent with therapeutic effect rimmed by viable cells of unknown histology (H&E; 40×). E, CW1757_X specimens grown directly in organoid format for the indicated culture periods in 6-well plates; scale bar, 1,000 μm. F, Kaplan–Meier survival analysis of mice bearing orthotopic xenografts from dissociated organoids originating from each tumor region in E. G, high-power micrograph of organoid-derived xenografted tumor tissue along the tumor–brain interface showing moderately increased cellular density and an indistinct tumor margin related to single-cell infiltration of tumor cells into the surrounding brain, a feature also found in the biopsy tissue (B; H&E; 40×). H, high-powered micrograph showing cellular density varying from moderate to high as detected by the variable amounts of basophilic nuclei and eosinophilic cytoplasm (H&E; 40×). I, high-power micrograph demonstrating a region of predominately high cellular density associated with hyperchromatic and pleomorphic basophilic nuclei, a region that differs markedly from the other regions of the tumor xenograft shown in G and H (H&E; 40×).

We next evaluated the presence of hypoxia within organoids using antibody detection of carbonic anhydrase IX (CA-IX), a functional hypoxic marker expressed by cells in response to low oxygen conditions (38). Hypoxic gradients were observed within the organoids (Fig. 4E'–G'), and strikingly, the presence of CA-IX immunofluorescence highly correlated with the spatial reduction of SOX2 expression (Fig. 4E''–G''). Although the frequency of $SOX2^+$ cells comparatively decreased crossing the hypoxic boundary, a minority of intensely $SOX2^+$ cells remained present among negative cells throughout hypoxic areas. Thus, the influence of hypoxia upon stem state in these conditions is large, but not absolute. Furthermore, multiple molecularly distinct $SOX2^+$ stem populations may be present within each organoid—one that requires high oxygen and growth factors to maintain its stem state (perhaps mimicking those in the perivascular niche), and one set that retains stem-like features despite resource-scarce microenvironmental conditions.

CSCs near the surface of organoids divide and die frequently, whereas hypoxic CSCs are quiescent

Stem state and hypoxia both influence cell division rates. We, therefore, evaluated the frequency of cell division across organoids using Ki-67 as a marker of proliferation. Proliferating cells were primarily localized near the organoid rim (Fig. 5A). Although most activity was observed in the periphery, rare CSCs in the hypoxic core also underwent division (Fig. 5B'). Although peripheral dividing cells were variably positive for SOX2 (Fig. 5B''), the rare core Ki-67^+ cells were typically strongly $SOX2^+$ (Fig. 5B', arrow). The apoptotic indicator cleaved caspase 3 was also comparatively frequent in the outer organoid rim (Fig. 5C–E), suggesting that this rapidly cycling cell population also has a higher turnover rate. In contrast, CSCs in the hypoxic core rarely cycle and rarely undergo apoptosis, reminiscent of a slow-cycling stem cell population, although accepted immunologic markers have yet to be described for such cells.

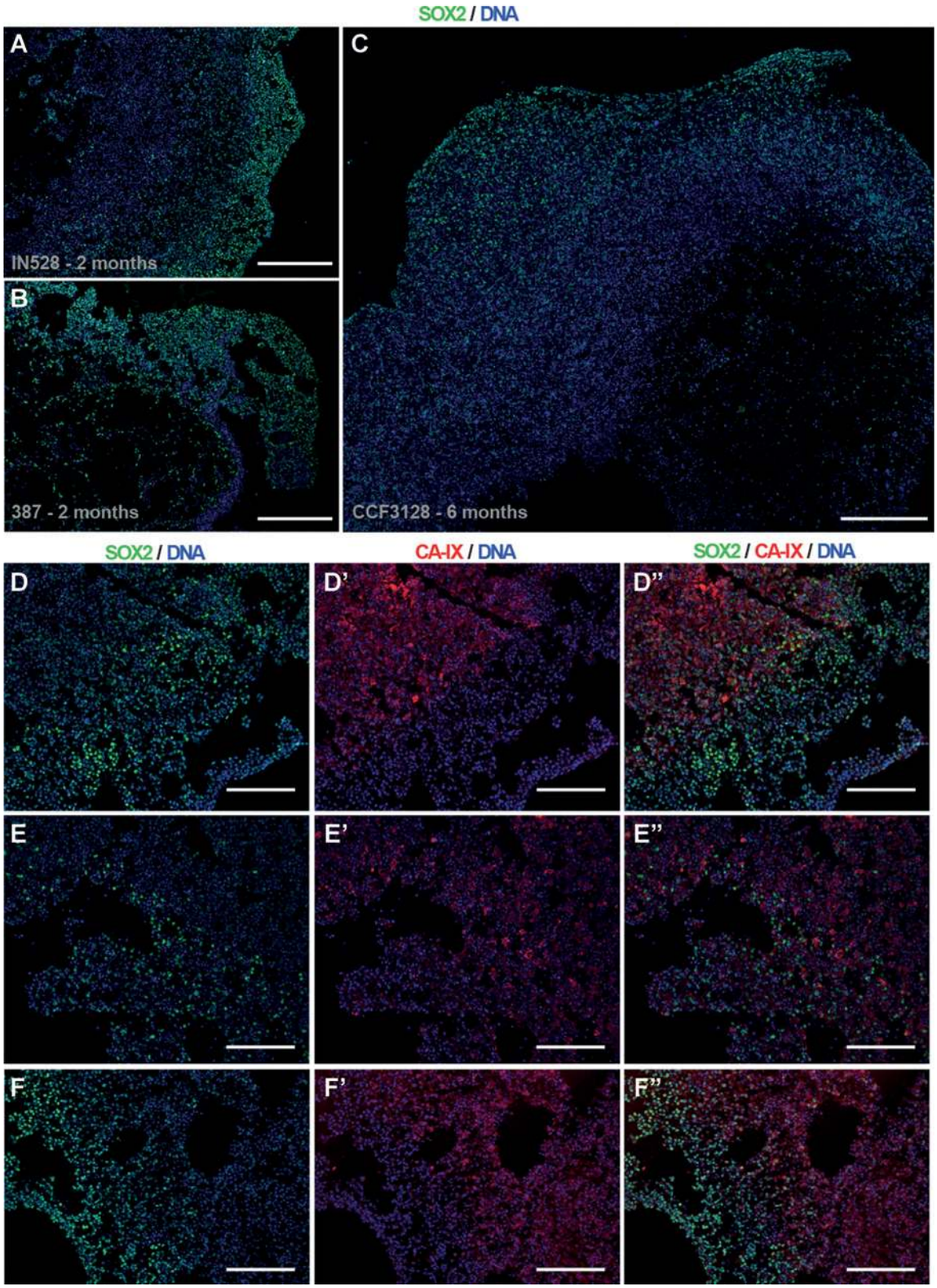

Figure 4.
Inverse gradients of stem cell frequency and hypoxia in organoids. A–C, widefield immunofluorescence imaging of nuclear SOX2 protein in IN528 (A), 387 (B), and CCF3128 (C, mosaic) organoids. Scale bars, 400 μm. D–F, coimmunofluorescence of SOX2 and CA-IX near the edges of IN528 organoids. Scale bars, 200 μm.

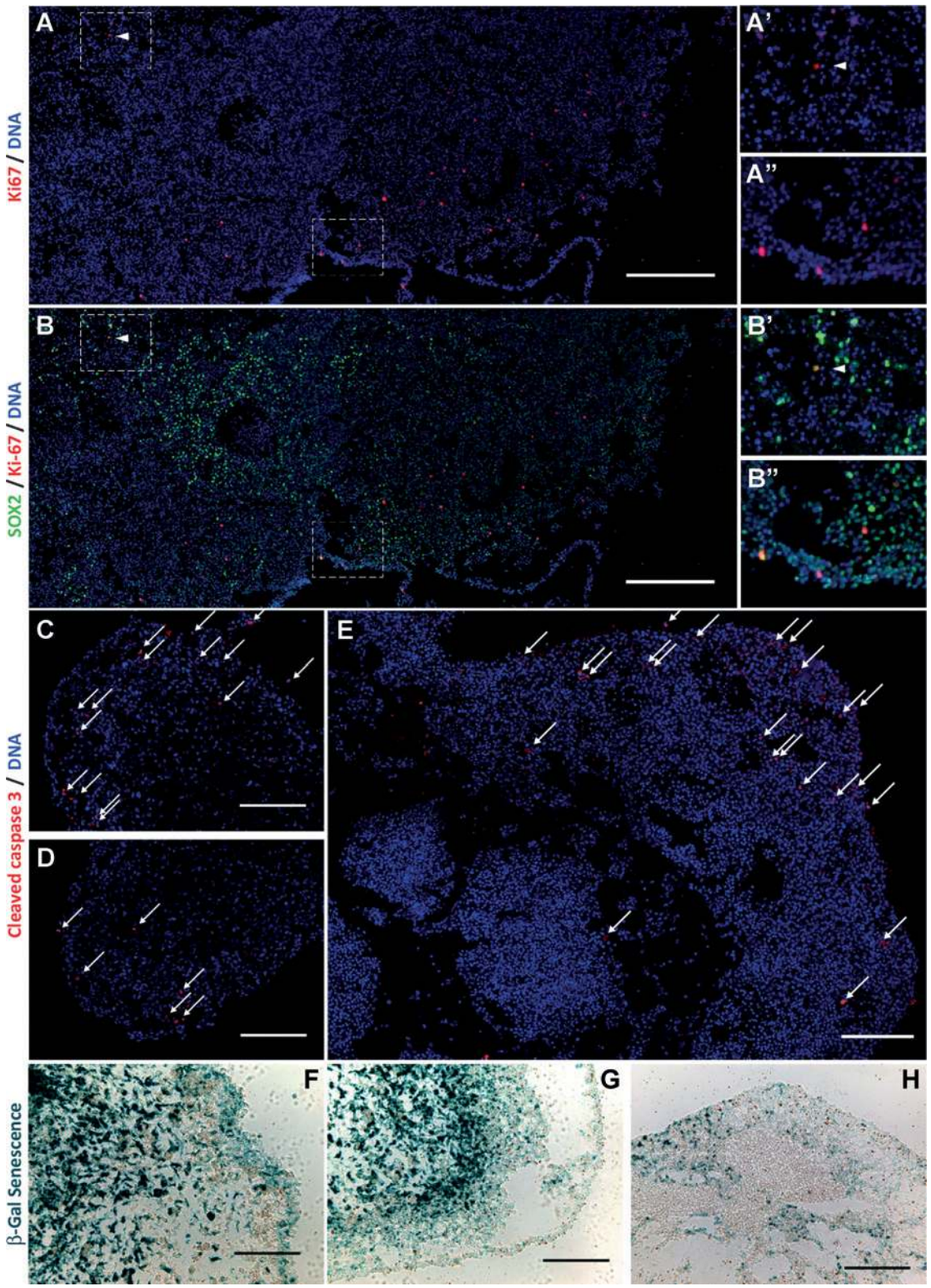

Figure 5.
Spatial and phenotypic cellular heterogeneity in organoids. A and B, immunofluorescence mosaic imaging of Ki-67 and SOX2 protein in IN528 organoids; scale bars, 400 μm. Insets (A′–B″) are magnified regions of the mosaic span as indicated by dashed boxes. C–E, immunofluorescence imaging specific to cleaved caspase 3 protein in IN528 (C and D) and 387 (E) organoids. White arrows, positive cells; scale bars, 200 μm. F–H, light micrographs of X-Gal detection of senescence-associated β-galactosidase in IN528 (F, G) and 387 (H) organoids. Scale bars, 100 μm (F), 200 μm (G), and 400 μm (H).

To complement proliferative rates, we also investigated cellular senescence within organoids. Although no reliable protein markers for senescence have been described in glioblastoma, the presence of beta-galactosidase (β-gal) activity (pH 6.5) is an indicator of senescence (39). X-gal staining marked β-gal–positive senescent cells present throughout tumor organoids (Fig. 5F–H). Senescent cells were most frequent throughout the inner hypoxic regions, but also present at a moderate frequency throughout the proliferative rim including at the outer edge. These results suggest that a cell's choice to become senescent is not simply a response to microenvironmental gradients but can also be made amidst proliferative stimuli. Thus, senescent cells can be maintained in organoid culture for months, enabling their study amidst proliferating cells that would overwhelm them in standard culture methods.

CSCs in organoids are radioresistant, whereas adjacent non-stem tumor cells are radiosensitive

Radiotherapy is a standard of care for glioblastoma patients, but CSCs are more resistant to radiation than their non-stem progeny (9). Glioblastoma organoids contain adjacent stem and non-stem cells and maintain tumor-like microenvironmental gradients. We therefore investigated whether heterogeneous radiation sensitivity is present throughout glioblastoma organoids. After irradiation, caspase 3 cleavage was significantly increased in glioblastoma cells around the organoid rim, but not within the organoid core (Fig. 6A, C, F). These apoptotic cells were also almost exclusively SOX2 negative (non-stem; Fig. 6D and G). These findings functionally validate the ability of $SOX2^+$ cells within the organoid to display a common CSC phenotype—radioresistance. They also demonstrate the potential for organoids to be used as a screening tool to identify sensitizers to standard-of-care therapies.

CSCs in organoids heterogeneously coexpress stem cell markers SOX2, OLIG2, and TLX

The perivascular and hypoxic CSC niches in brain tumors display distinct molecular regulation (30). Our findings suggest that there may be molecularly and functionally distinct $SOX2^+$ CSC populations within organoids. We therefore investigated the coexpression of additional stem cell markers potentially important in CSC biology. The orphan nuclear receptor tailless (TLX) is a mediator of self-renewal and long-term proliferation of embryonic and neural stem cells (NSC) and may be critical in the initiation of glioma (40, 41). In a genetically engineered mouse model, TLX plays an essential role in gliomagenesis and may mark a quiescent CSC population, distinct from the $SOX2^+$ cells, which are proliferative (42, 43). Based on these findings, we investigated whether TLX was differentially expressed within potential slow-cycling CSCs of the hypoxic core. Surprisingly, rather than marking rare hypoxic cells, TLX immunofluorescence was nearly universal among SOX2-positive cells (Fig. 7A–A'''). TLX and SOX2 staining overwhelmingly coincided in the proliferative rim, hypoxic core, and in CSC nests among differentiated tumor cells (Fig. 7A'–7A'''). This suggests that TLX function may be distinct in human gliomas compared with previous mouse models. The correspondence between TLX and SOX2 expression in CSCs parallels other work in adult NSCs showing a transcriptional network where SOX2 directly regulates TLX transcription and TLX and SOX2 form transcription complex at TLX-controlled genes (44). In light of these data, our staining pattern suggests that the SOX2 and TLX regulatory networks in our CSCs may have similarities to TLX regulation in adult NSCs.

The basic helix-loop-helix transcription factor OLIG2 controls replication competence in NSCs and glioblastoma, is preferentially expressed in CSCs, is required for glioblastoma initiation in mouse models, and is one of four factors capable of reprograming glioma cells to a CSC state (36, 45, 46). CSC tumorspheres are almost universally positive for SOX2 and for OLIG2 (Supplementary Fig. S4A–S4D). We investigated whether OLIG2 is coexpressed with SOX2 in organoids and found that such coexpression is common in both inner and outer organoid regions, but to varying degrees (Fig. 7B–D; Supplementary Fig. S4E). In the CSC-rich proliferative rim, the vast majority of cells coexpressed OLIG2 and SOX2 (Fig. 7D''). SOX2/OLIG2 double-positive cells were still frequent amongst CSCs in the hypoxic core, but strongly single-positive cells were frequently present as well (Fig. 7D'). Once away from the proliferative rim, this heterogeneity extends deep within the organoids (Supplementary Fig. S5). These findings suggest that separate organoid regions may harbor distinct but overlapping CSC subpopulations.

Discussion

Three-dimensional organoid culture systems permit a complex structure to develop, mimicking organ development (21, 26, 29). Although some cancers display spatial orientation relative to the stem cell niche, gliomas generate neo-niches that lack coherent organization. We investigated the spatial distribution of CSCs within organoids and observed, similar to patient tumors, little evidence of self-organization or higher-level patterning. Small stem cell nests were present in some organoid cultures (Fig. 7A'''; Supplementary Fig. S4E), but gradients of stem cell markers appear primarily driven by resource diffusion with SOX2-positive cells densely located near the organoid periphery with the highest exposure to oxygen, nutrients, and media growth factors. This region could be viewed as the *in vitro* equivalent of the perivascular niche, whereas the organoid interior is a mimic of the resource-poor hypoxic niche *in vivo*. This analogy is supported by the inverse relationship between $SOX2^+$ frequency and regions staining for the functional hypoxic marker CA-IX (Fig. 4D–F). Interestingly, this gradient is not linear. Although markedly fewer cells are $SOX2^+$ within hypoxic regions, the punctate distribution of strongly $SOX2^+$ cells remained throughout the organoid interior (Supplementary Fig. S5). This inverse relationship of markers from rim to center combined with clear nuclear localization of the SOX2 transcription factor shows that these results are not a technical artifact, such as "edge effect" or incomplete fixation. This biologic relationship suggests a cellular choice driven by a threshold rather than a simple reflection of resource diffusion.

We further investigated the relationship between SOX2 and expression of another key glioma stem cell gene, OLIG2 (36, 45, 46). Overlap between SOX2 and OLIG2 expression is particularly prominent in the proliferative rim of glioblastoma organoids, whereas CSCs in the core are more heterogeneous in their expression or coexpression of these CSC markers (Fig. 7B–D). This suggests that tumor organoids may harbor distinct molecular subpopulations within the stem cell hierarchy and that the distribution of these cells may be influenced by their microenvironment. We see similar stem cell behavior in tumors *in vivo* where CSCs are enriched within perivascular niches yet also reside in hypoxic niches far from the vasculature. The microenvironmental

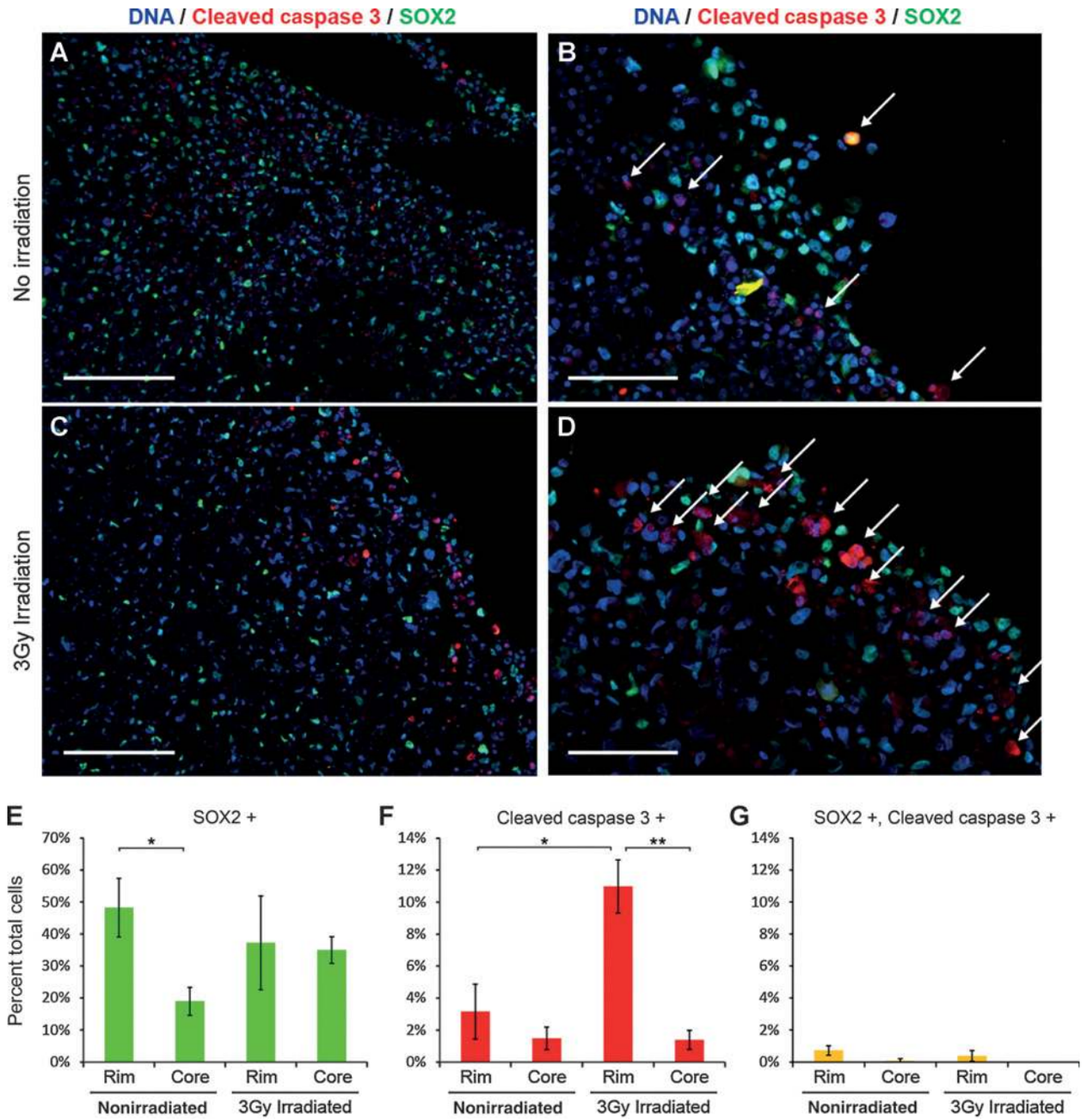

Figure 6.
Organoid rim non-CSCs are radiosensitive. A–D, immunofluorescence imaging of cleaved caspase 3 protein and SOX2 protein in IN528 organoids 96 hours after 3 Gy irradiation. White arrows, cleaved caspase 3–positive cells. Scale bars, 200 μm (A, C) or 100 μm (B, D). E–G, total cells and cells positive for SOX2 (E), cleaved caspase 3 (F), and both (G) were blindly counted from three nonoverlapping high-power fields within the indicated organoid regions. Student *t* test; *, $P < 0.02$; **, $P < 0.001$.

gradients present in organoids allow similar heterogeneity of CSCs growing simultaneously. The molecular profiles of these CSC subtypes as well as their influence upon each other and their non-stem glioblastoma cell neighbors *in vivo* or in organoid culture have yet to be determined.

NSCs are long-lived and quiescent with the proliferative burden arising from more lineage-committed transit-amplifying cells. In contrast, in most cell culture methods including neural stem cell and glioblastoma stem cell cultures, rapidly proliferating populations outcompete slow-cycling, quiescent, or senescent cells. The influence of these populations in scientific experiments is thus limited. In organoids, the vast majority of proliferative activity (as determined by Ki-67 staining) was localized to the peripheral rim (Fig. 5A). This is not surprising as this region contains the highest levels of growth factors, oxygen, and nutrients, all of which are required for proliferative activity. These cells are variably positive

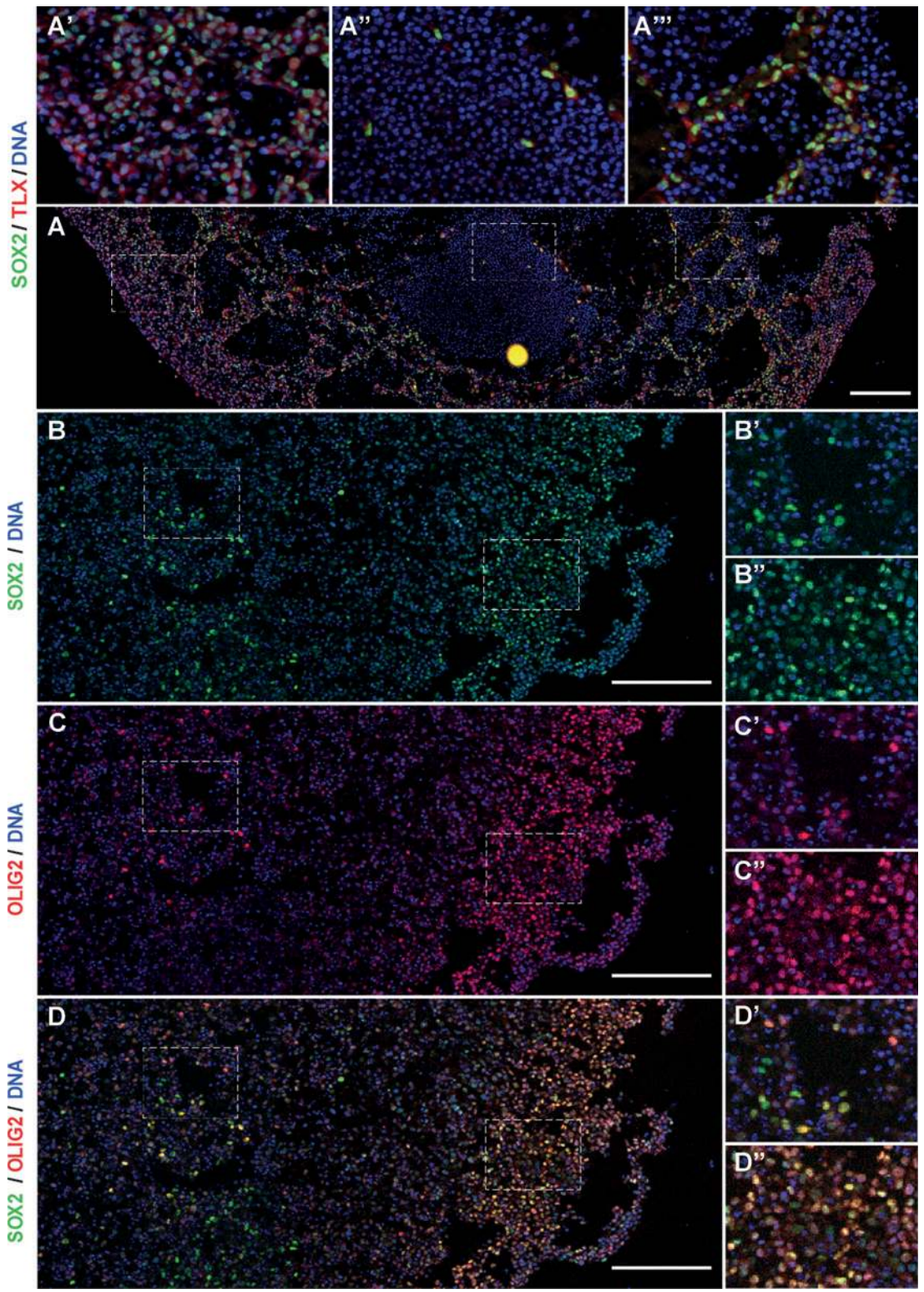

Figure 7.
Partially overlapping stem cell marker expression in glioblastoma organoids. A, immunofluorescence mosaic imaging of SOX2 and TLX protein in 387 organoids. Scale bars, 200 μm. Insets (A′–A‴) are magnified regions of the mosaic span as indicated by dashed boxes. B–D, immunofluorescence mosaic imaging of SOX2 and OLIG2 protein expression in IN528 organoids. Insets (B′–D″) are magnified regions of the mosaic span as indicated by dashed boxes. Scale bars, 200 μm.

for the stem cell marker SOX2, suggesting the proliferation of both stem-like and more differentiated (such as transit-amplifying) cell populations in this region (Fig. 5B''). A rare population of $SOX2^+$ cells in the hypoxic core also showed clear Ki-67 positivity (Fig. 5B'). Furthermore, staining for cleaved caspase 3 revealed relatively high apoptotic rates in the organoid periphery compared with the core (Fig. 5C–E). This suggests that the proliferative edge is a region of high cell turnover surrounding a more stable core, rather than the presence of a conveyor-belt–like effect from edge proliferation to core death.

Cytotoxic cancer therapies may be less effective in slower cycling or nonproliferative cancer cells. The above finding may indicate a long-lived population of $SOX2^+$ cells in the core that have retained the ability to divide but do so very infrequently, as would be expected for a slow-cycling or quiescent stem cell. The presence of senescent glioblastoma cells, in concert with the potential presence of quiescent CSCs, in tumor organoids suggests that organoids may reflect greater complexity of heterogeneous tumor cell populations compared with other culture techniques. For instance, we have demonstrated radiosensitive non-stem cells and radioresistant CSCs growing adjacently within the organoid rim (Fig. 6). This preserved heterogeneity underscores a potential utility of organoids derived directly from patients for screening assays, the study of therapies and therapeutic resistance, and in the development of patient avatar models.

We have shown the striking ability of organoid-derived xenografts from multiple patient samples and tumor regions to recapitulate the single-cell infiltrative phenotype of the original patient tumor (Fig. 2H, K, N; Fig. 3G–I), whereas tumorsphere-derived xenografts produce a solid mass (Fig. 2I, L, O). This finding suggests that organoid culture may preserve a patient tumor cell population capable of reproducing this infiltrative phenotype. Organoid culture may therefore be essential to recapitulate and study this deadly component of glioblastoma. Infiltrative mouse xenografts derived from organoids and solid xenograft tumors derived from tumorspheres may also have different responses to candidate therapeutics. Parallel organoid- and tumorsphere-derived xenograft animals may therefore complement each other in preclinical trials.

Organoid growth has a different spectrum of benefits and drawbacks compared with tumorspheres or to xenografts (Supplementary Table S1). Organoids are more time consuming at the time of establishment than tumorspheres and may be impractical for high-throughput screening efforts. Compared with tumorspheres, organoids have low and regionally variable cellular growth rates. Also in contrast with traditional culture methods, the cellular heterogeneity present in organoids could obscure molecular responses to experimental perturbations if the organoid is lysed in bulk prior to analysis (i.e., for immunoblot or qPCR assay).

The cellular and microenvironmental heterogeneity within tumor organoids enables the simultaneous culture of functionally and phenotypically diverse stem and non-stem glioblastoma cell populations. Neither *in vivo* xenograft propagation nor any currently described culture systems can similarly pair such cellular diversity and microenvironmental gradients with the experimental control of *in vitro* culture. Organoid culture may allow the study of stem and non-stem glioblastoma cell populations in the same culture, the investigation of interactions between CSCs in proliferative and hypoxic niches, and the further dissection of subpopulations within the glioblastoma stem cell hierarchy. Future studies utilizing organoids may empower medium-throughput drug screening with the ability to detect mixed responses that are often discovered only in clinical trials. Combinatorial studies in organoid format may circumvent the feasibility barrier posed by *in vivo* studies. The creation of organoids may permit more reliable models for precision medicine, even from tumor types such as like cerebral metastases that are challenging to perpetuate. Finally, genetically engineered organoids have been developed to interrogate the genetic initiation and progression of tumors in the gastrointestinal system (47). Our studies suggest such models are feasible in brain tumors as well.

Disclosure of Potential Conflicts of Interest

No potential conflicts of interest were disclosed.

Authors' Contributions

Conception and design: C.G. Hubert, M. Rivera, R.E. McLendon, A.E. Sloan, J.N. Rich

Development of methodology: C.G. Hubert, M. Rivera

Acquisition of data (provided animals, acquired and managed patients, provided facilities, etc.): C.G. Hubert, M. Rivera, L.C. Spangler, Q. Wu, S.C. Mack, B.C. Prager, M. Couce, A.E. Sloan

Analysis and interpretation of data (e.g., statistical analysis, biostatistics, computational analysis): C.G. Hubert, S.C. Mack, B.C. Prager, R.E. McLendon, J.N. Rich

Writing, review, and/or revision of the manuscript: C.G. Hubert, S.C. Mack, R.E. McLendon, A.E. Sloan, J.N. Rich

Administrative, technical, or material support (i.e., reporting or organizing data, constructing databases): L.C. Spangler, Q. Wu, S.C. Mack, A.E. Sloan, J.N. Rich

Study supervision: A.E. Sloan, J.N. Rich

Acknowledgments

The authors thank funding sources and members of the Rich Lab for their support, the Cleveland Clinic Imaging, Histology, and Flow Cytometry Cores and Biological Resources Unit for their assistance and technical expertise, and the laboratory of Justin Lathia for the gift of the RCAS-GFAP-tva/PDGFB cell culture.

Grant Support

This work was supported by The NIH grants CA189647 (C.G. Hubert), CA154130, CA171652, CA169117, NS087913, NS089272, CA197718 (J.N. Rich), Research Programs Committees of Cleveland Clinic (J.N. Rich), and James S. McDonnell Foundation (J.N. Rich). A.E. Sloan is supported by the Peter D. Cristal Chair in Neurosurgical Oncology as well as the Kimble endowment for Neurosurgical Oncology. S.C. Mack is supported by a CIHR Banting Fellowship.

The costs of publication of this article were defrayed in part by the payment of page charges. This article must therefore be hereby marked *advertisement* in accordance with 18 U.S.C. Section 1734 solely to indicate this fact.

Received September 8, 2015; revised January 7, 2016; accepted January 25, 2016; published OnlineFirst February 19, 2016.

References

1. Stupp R, Hegi ME, Mason WP, van den Bent MJ, Taphoorn MJ, Janzer RC, et al. Effects of radiotherapy with concomitant and adjuvant temozolomide versus radiotherapy alone on survival in glioblastoma in a randomised phase III study: 5-year analysis of the EORTC-NCIC trial. Lancet Oncol 2009;10:459–66.

2. Lathia JD, Heddleston JM, Venere M, Rich JN. Deadly teamwork: Neural cancer stem cells and the tumor microenvironment. Cell Stem Cell 2011;8:482–5.
3. Meyer M, Reimand J, Lan X, Head R, Zhu X, Kushida M, et al. Single cell-derived clonal analysis of human glioblastoma links functional and genomic heterogeneity. Proc Natl Acad Sci U S A 2015;112:851–6.
4. Patel AP, Tirosh I, Trombetta JJ, Shalek AK, Gillespie SM, Wakimoto H, et al. Single-cell RNA-seq highlights intratumoral heterogeneity in primary glioblastoma. Science 2014;344:1396–401.
5. Vescovi AL, Galli R, Reynolds BA. Brain tumour stem cells. Nat Rev 2006; 6:425–36.
6. Galli R, Binda E, Orfanelli U, Cipelletti B, Gritti A, De Vitis S, et al. Isolation and characterization of tumorigenic, stem-like neural precursors from human glioblastoma. Cancer Res 2004;64:7011–21.
7. Singh SK, Hawkins C, Clarke ID, Squire JA, Bayani J, Hide T, et al. Identification of human brain tumour initiating cells. Nature 2004;432: 396–401.
8. Hemmati HD, Nakano I, Lazareff JA, Masterman-Smith M, Geschwind DH, Bronner-Fraser M, et al. Cancerous stem cells can arise from pediatric brain tumors. Proc Natl Acad Sci U S A 2003;100:15178–83.
9. Bao S, Wu Q, McLendon RE, Hao Y, Shi Q, Hjelmeland AB, et al. Glioma stem cells promote radioresistance by preferential activation of the DNA damage response. Nature 2006;444:756–60.
10. Calabrese C, Poppleton H, Kocak M, Hogg TL, Fuller C, Hamner B, et al. A perivascular niche for brain tumor stem cells. Cancer Cell 2007;11:69–82.
11. Li Z, Bao S, Wu Q, Wang H, Eyler C, Sathornsumetee S, et al. Hypoxia-inducible factors regulate tumorigenic capacity of glioma stem cells. Cancer Cell 2009;15:501–13.
12. Seidel S, Garvalov BK, Wirta V, von Stechow L, Schanzer A, Meletis K, et al. A hypoxic niche regulates glioblastoma stem cells through hypoxia inducible factor 2 alpha. Brain 2010;133:983–95.
13. Bar EE, Lin A, Mahairaki V, Matsui W, Eberhart CG. Hypoxia increases the expression of stem-cell markers and promotes clonogenicity in glioblastoma neurospheres. Am J Pathol 2010;177:1491–502.
14. Yan K, Wu Q, Yan DH, Lee CH, Rahim N, Tritschler I, et al. Glioma cancer stem cells secrete Gremlin1 to promote their maintenance within the tumor hierarchy. Genes Dev 2014;28:1085–100.
15. Charles N, Ozawa T, Squatrito M, Bleau AM, Brennan CW, Hambardzumyan D, et al. Perivascular nitric oxide activates notch signaling and promotes stem-like character in PDGF-induced glioma cells. Cell Stem Cell 2010;6:141–52.
16. Zhu TS, Costello MA, Talsma CE, Flack CG, Crowley JG, Hamm LL, et al. Endothelial cells create a stem cell niche in glioblastoma by providing NOTCH ligands that nurture self-renewal of cancer stem-like cells. Cancer Res 2011;71:6061–72.
17. Wang H, Lathia JD, Wu Q, Wang J, Li Z, Heddleston JM, et al. Targeting interleukin 6 signaling suppresses glioma stem cell survival and tumor growth. Stem Cells (Dayton, Ohio) 2009;27:2393–404.
18. Bao S, Wu Q, Sathornsumetee S, Hao Y, Li Z, Hjelmeland AB, et al. Stem cell-like glioma cells promote tumor angiogenesis through vascular endothelial growth factor. Cancer Res 2006;66:7843–8.
19. Cheng L, Huang Z, Zhou W, Wu Q, Donnola S, Liu JK, et al. Glioblastoma stem cells generate vascular pericytes to support vessel function and tumor growth. Cell 2013;153:139–52.
20. Becher OJ, Holland EC. Genetically engineered models have advantages over xenografts for preclinical studies. Cancer Res 2006;66:3355–8, discussion 58–9.
21. Shamir ER, Ewald AJ. Three-dimensional organotypic culture: Experimental models of mammalian biology and disease. Nat Rev Mol Cell Biol 2014;15:647–64.
22. Boj SF, Hwang CI, Baker LA, Chio II, Engle DD, Corbo V, et al. Organoid models of human and mouse ductal pancreatic cancer. Cell 2015;160: 324–38.
23. McCracken KW, Cata EM, Crawford CM, Sinagoga KL, Schumacher M, Rockich BE, et al. Modelling human development and disease in pluripotent stem-cell-derived gastric organoids. Nature 2014;516: 400–4.
24. Smith SJ, Wilson M, Ward JH, Rahman CV, Peet AC, Macarthur DC, et al. Recapitulation of tumor heterogeneity and molecular signatures in a 3D brain cancer model with decreased sensitivity to histone deacetylase inhibition. PLoS One 2012;7:e52335.
25. Lancaster MA, Knoblich JA. Generation of cerebral organoids from human pluripotent stem cells. Nat Protoc 2014;9:2329–40.
26. Lancaster MA, Renner M, Martin CA, Wenzel D, Bicknell LS, Hurles ME, et al. Cerebral organoids model human brain development and microcephaly. Nature 2013;501:373–9.
27. Gao D, Vela I, Sboner A, Iaquinta PJ, Karthaus WR, Gopalan A, et al. Organoid cultures derived from patients with advanced prostate cancer. Cell 2014;159:176–87.
28. Karthaus WR, Iaquinta PJ, Drost J, Gracanin A, van Boxtel R, Wongvipat J, et al. Identification of multipotent luminal progenitor cells in human prostate organoid cultures. Cell 2014;159:163–75.
29. Sato T, Vries RG, Snippert HJ, van de Wetering M, Barker N, Stange DE, et al. Single Lgr5 stem cells build crypt-villus structures in vitro without a mesenchymal niche. Nature 2009;459:262–5.
30. Mohyeldin A, Garzon-Muvdi T, Quinones-Hinojosa A. Oxygen in stem cell biology: a critical component of the stem cell niche. Cell Stem Cell 2010; 7:150–61.
31. Joo KM, Kim J, Jin J, Kim M, Seol HJ, Muradov J, et al. Patient-specific orthotopic glioblastoma xenograft models recapitulate the histopathology and biology of human glioblastomas in situ. Cell Rep 2013;3:260–73.
32. Cloughesy TF, Cavenee WK, Mischel PS. Glioblastoma: from molecular pathology to targeted treatment. Annu Rev Pathol 2014;9:1–25.
33. Flavahan WA, Wu Q, Hitomi M, Rahim N, Kim Y, Sloan AE, et al. Brain tumor initiating cells adapt to restricted nutrition through preferential glucose uptake. Nat Neurosci 2013;16:1373–82.
34. Young RA. Control of the embryonic stem cell state. Cell 2011;144: 940–54.
35. Takahashi K, Yamanaka S. Induction of pluripotent stem cells from mouse embryonic and adult fibroblast cultures by defined factors. Cell 2006; 126:663–76.
36. Suva ML, Rheinbay E, Gillespie SM, Patel AP, Wakimoto H, Rabkin SD, et al. Reconstructing and reprogramming the tumor-propagating potential of glioblastoma stem-like cells. Cell 2014;157:580–94.
37. de la Rocha AM, Sampron N, Alonso MM, Matheu A. Role of SOX family of transcription factors in central nervous system tumors. Am J Cancer Res 2014;4:312–24.
38. Potter C, Harris AL. Hypoxia inducible carbonic anhydrase IX, marker of tumour hypoxia, survival pathway and therapy target. Cell Cycle (Georgetown, Tex 2004;3:164–7.
39. Dimri GP, Lee X, Basile G, Acosta M, Scott G, Roskelley C, et al. A biomarker that identifies senescent human cells in culture and in aging skin in vivo. Proc Natl Acad Sci U S A 1995;92:9363–7.
40. Qu Q, Sun G, Li W, Yang S, Ye P, Zhao C, et al. Orphan nuclear receptor TLX activates Wnt/beta-catenin signalling to stimulate neural stem cell proliferation and self-renewal. Nat Cell Biol 2010;12:31–40; sup pp 1–9.
41. Zou Y, Niu W, Qin S, Downes M, Burns DK, Zhang CL. The nuclear receptor TLX is required for gliomagenesis within the adult neurogenic niche. Mol Cell Biol 2012;32:4811–20.
42. Liu HK, Wang Y, Belz T, Bock D, Takacs A, Radlwimmer B, et al. The nuclear receptor tailless induces long-term neural stem cell expansion and brain tumor initiation. Genes Dev 2010;24:683–95.
43. Zhu Z, Khan MA, Weiler M, Blaes J, Jestaedt L, Geibert M, et al. Targeting self-renewal in high-grade brain tumors leads to loss of brain tumor stem cells and prolonged survival. Cell Stem Cell 2014;15:185–98.
44. Shimozaki K, Zhang CL, Suh H, Denli AM, Evans RM, Gage FH. SRY-box-containing gene 2 regulation of nuclear receptor tailless (Tlx) transcription in adult neural stem cells. J Biol Chem 2012;287:5969–78.
45. Ligon KL, Huillard E, Mehta S, Kesari S, Liu H, Alberta JA, et al. Olig2-regulated lineage-restricted pathway controls replication competence in neural stem cells and malignant glioma. Neuron 2007;53:503–17.
46. Mehta S, Huillard E, Kesari S, Maire CL, Golebiowski D, Harrington EP, et al. The central nervous system-restricted transcription factor Olig2 opposes p53 responses to genotoxic damage in neural progenitors and malignant glioma. Cancer Cell 2011;19:359–71.
47. Matano M, Date S, Shimokawa M, Takano A, Fujii M, Ohta Y, et al. Modeling colorectal cancer using CRISPR-Cas9-mediated engineering of human intestinal organoids. Nat Med 2015;21:256–62.